Equilibrium free energy measurement of a confined electron driven out of equilibrium

A. Hofmann,* V. F. Maisi, C. Rössler, J. Basset, T. Krähenmann, P. Märki, T. Ihn, K. Ensslin, C. Reichl, and W. Wegscheider
Solid State Physics Laboratory, ETH Zürich, 8093 Zürich, Switzerland
(Received 20 April 2015; revised manuscript received 2 November 2015; published 15 January 2016)

The Jarzynski equality relates nonequilibrium thermodynamics and equilibrium states. We realize a coupled quantum dot-electron reservoir system in which the time resolved observation of the tunneling dynamics is used to explicitly measure the exerted work and dissipated heat per single charge. We determine accurate values of the equilibrium free energy change over a large range of final state energies by driving the system far from equilibrium.

DOI: 10.1103/PhysRevB.93.035425

I. INTRODUCTION

Equilibrium thermodynamics makes predictions for macroscopic many-particle systems independent of detailed microscopic processes governing their properties. As systems become smaller, fluctuations departing from the equilibrium state often become prominent, and nonequilibrium dynamics needs to be taken into account. The discovery of fluctuation relations [1,2] and their experimental tests [3–13] are major steps towards understanding the nonequilibrium statistical behavior of small systems down to the atomic level.

The Jarzynski equality (JE) states that in a classical thermodynamic system subject to an arbitrary drive protocol, the performed work ΔW during driving satisfies [1]

$$\left\langle \exp\left(-\frac{\Delta W}{kT}\right)\right\rangle = \exp\left(-\frac{\Delta F}{kT}\right), \tag{1}$$

where the average is taken over different repetitions of the drive protocol, and $\Delta F/kT$ is the ratio of the equilibrium free energy difference between the initial and final state of the drive and the thermal energy.

In a pioneering set of experiments, Collin [3] and Liphardt [5] investigated the reversible and irreversible stretching of a single molecule of ribonucleic acid (RNA) to determine the free energy in systems where precise calculations are difficult to obtain. Using superconducting nanostructures, Saira and coworkers [4] tested the JE in systems involving many energy levels and for the special case of zero free energy.

Here, we study a discrete energy level in a semiconductor quantum dot coupled to a single thermal and electron reservoir. We demonstrate experimentally the connection of the free energy, being an equilibrium quantity, to the nonequilibrium dynamics as predicted by the JE [1] by driving the quantum dot out of equilibrium with respect to the reservoir. In addition to the results presented in Ref. [4], our experiment tests the JE for a range of free energy values which can be tuned by suitable gate voltages. We show that quantum dot systems are good testbeds for studying thermodynamics on the level of single electrons. At a general level, we demonstrate experimentally that the free energy can be measured even far from equilibrium by utilizing the JE. The free energy is a direct measure of the maximum work that may be extracted from a reversible process or the minimum work which needs to be invested to activate it [14]. Knowledge of the free energy is important for experiments where drive is applied in order to cool the system, or to retrieve information about system properties, as well as for Szilard's engine and Maxwell's demon experiments.

II. RESULTS

A. Equilibrium characterization

We first characterize the quantum dot (QD)-reservoir system in thermodynamic equilibrium. The device used is shown in Fig. 1(a). A GaAs/AlGaAs heterostructure is grown to confine electrons in a plane perpendicular to the growth direction. Negative voltages applied to top gates patterned on the surface of the crystal control the additional lateral confinement within this two-dimensional electron gas (2DEG) and form a QD [15]. The QD couples to a large contact region of the 2DEG acting as the electron and heat reservoir characterized by a Fermi distribution at temperature $T \approx 40$ mK. The voltage V_{PG} applied to the plunger gate controls the confinement potential and thereby shifts the electronic states of the quantum dot in energy, providing a handle to the number of states below the Fermi energy of the reservoir. We use V_{PG} to decrease the size of the QD until only a single occupied energy level remains, the "last electron" [16,17]. The gate labeled "charge detector" in Fig. 1(a) controls an additional quantum point contact in close vicinity of the QD. Its conductance is set to a value between zero and the first conductance plateau, where it is sensitive to changes of the QD charge state through capacitive coupling [18,19].

A typical time trace of the charge detector current is presented in Fig. 2(a). The two levels indicate the number of charges residing in the QD ("out" and "in" correspond to 0 or 1 electron, respectively). We extract the times $t^{(i)}_{\mathrm{in/out}}$ during which the QD energy state is occupied ("in") or empty ("out") and estimate its occupation probabilities $\tilde{f}_{\mathrm{in/out}}$ and the tunnel rates $W_{\mathrm{in/out}}$ [18–20] using

$$W_{\mathrm{in/out}} = \frac{1}{\langle t_{\mathrm{out/in}}\rangle}; \quad \tilde{f}_{\mathrm{in/out}} = \frac{W_{\mathrm{in/out}}}{W_{\mathrm{in}} + W_{\mathrm{out}}}, \tag{2}$$

where $\langle\cdot\rangle$ denotes the average over a time trace. In Fig. 2(b) we present $\tilde{f}_{\mathrm{in/out}}(E)$ and $W_{\mathrm{in/out}}(E)$ extracted from time traces at a range of plunger gate energies E, with E as defined in Fig. 1(b).

Within a model description, Fermi's golden rule describes electron tunneling with an energy-independent tunnel coupling

*andrea.hofmann@phys.ethz.ch

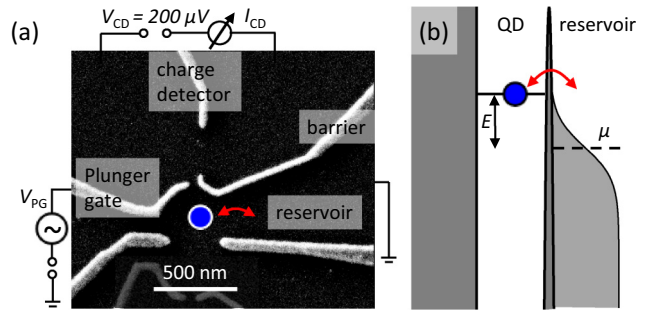

FIG. 1. The device used in the experiments described in the text together with an energy diagram showing a single tunneling event. (a) Scanning electron micrograph of the device formed on a GaAs/AlGaAs heterostructure with a 2DEG 90 nm below the surface (dark gray area). Ti/Au gates (bright fingers) are patterned with electron-beam lithography to capacitively deplete the 2DEG. The QD is formed in the place indicated by the blue circle and is tunnel coupled to a reservoir, as shown by the red arrow, while the other barrier is fully closed. An arbitrary waveform generator is connected to the plunger gate to drive the QD. (b) An energy diagram indicates a tunneling process between the QD and the lead reservoir at energy E measured from the Fermi energy μ.

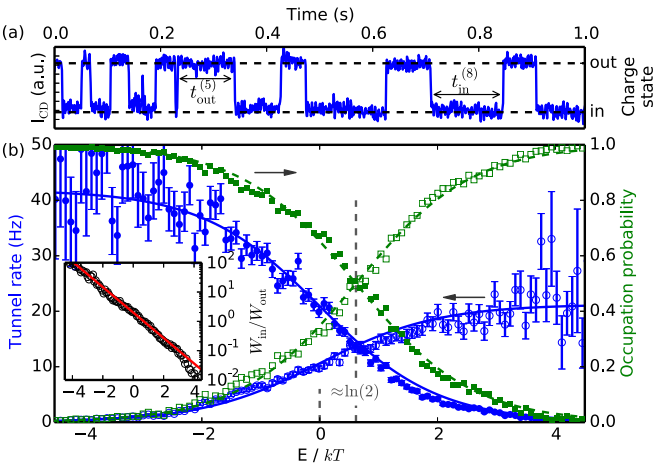

FIG. 2. Time trace of the charge detector signal showing single electron tunneling events as well as the extracted tunnel frequency and occupation probability. (a) A typical time trace of the charge detector current (I_{CD}). The current oscillates around 4 nA, and the difference in current between the two states is ≈100 pA. (b) Tunnel rates (filled blue for tunneling in and open blue dots for tunneling out) and occupation probabilities (green squares, filled for occupied and empty for nonoccupied) extracted from CD time traces of 60 s. The abscissa is the negative plunger gate voltage measured from the Fermi energy and scaled by the temperature, $T = 223$ μV in units of V_{PG}. The error bars indicate statistical errors assuming Gaussian fluctuations. The solid blue lines are weighted least-mean-square fits to Eq. (2), from which $\Gamma_{in} = 41.8 \pm 1.6$ Hz and $\Gamma_{out} = 21.2 \pm 0.6$ Hz and the temperature are determined. The dashed green lines are fits to Eq. (4). Inset: The ratio of the two tunnel rates (black circles) is plotted as a function of energy from μ, together with the exponential behavior as expected from the detailed balance condition (red line).

constant Γ. The Fermi distribution $f(E,T)$ describes the lead occupation at an energy E measured from the Fermi energy μ. For an empty d-fold degenerate energy level, the tunneling rate into this level is the sum of the tunneling rates into either of the degenerate states. Tunneling out occurs only from the single state which has been occupied. This leads to

$$W_{in}(E) = d\Gamma f(E,T) = \Gamma_{in} f(E,T) \tag{3a}$$

$$W_{out}(E) = \Gamma(1 - f(E,T)) = \Gamma_{out} f(-E,T). \tag{3b}$$

In equilibrium, the occupation probabilities $\tilde{f}_{in/out}$ of the d-fold degenerate QD energy state are described by the partition sum $Z(E)$ [14] according to

$$Z(E) = 1 + de^{-\frac{E}{kT}} = 1 + e^{-\frac{E-E_d}{kT}}, \text{ with } E_d = kT\ln(d) \tag{4}$$

$$\tilde{f}_{in} = \frac{de^{-\frac{E}{kT}}}{Z} = f(E - E_d),\ \tilde{f}_{out} = \frac{1}{Z} = 1 - f(E - E_d). \tag{5}$$

We extract the tunnel coupling constants, the electrochemical potential $\mu = 0$ (used as the zero-energy reference), as well as the temperature of the reservoir in units of plunger gate voltage from a weighted least-mean-square fit of the data in Fig. 2(b) (solid blue line) to Eqs. (3). We find tunnel coupling constants $\Gamma_{in} = 41.8 \pm 1.6$ Hz and $\Gamma_{out} = 21.2 \pm 0.6$ Hz. This implies a degeneracy $d = \Gamma_{in}/\Gamma_{out} = 1.97 \pm 0.04$, in agreement with the spin-degeneracy $d = 2$ expected for the last electron, where only the lowest orbital plays a role [17,21,22] and the degeneracy is due to spin only. The dashed green lines in Fig. 2(b) are least-mean-square fits of the experimental occupation probabilities $\tilde{f}_{in/out}$ to Eq. (4). Here, the fit parameters are the temperature and the energy offset E_d. We find $E_d/kT = 0.62 \pm 0.08$, in agreement with $E_d/kT = \ln(2)$ for a twofold degenerate energy state. From the fits to the tunnel rates and the occupation probabilities, we recover the same value for the temperature. The system obeys the detailed balance condition for the tunneling rates, $W_{in}/W_{out} = d\exp(-E/kT)$ for $d = 2$, as shown in the inset of Fig. 2(b).

B. Free energy measurement out of equilibrium

After having characterized the QD-reservoir system in equilibrium, our goal is to measure the equilibrium free energy change ΔF of the QD between an initial and a final state differing by a value $\Delta E \propto -V_{PG}$. To this end we drive the QD out of equilibrium by applying a time-dependent plunger gate voltage $V_{PG}(t)$. The Jarzynski equality, given in Eq. (1), provides the necessary tools for such an experiment: As the work can be evaluated for nonequilibrium situations, the JE allows us to determine the equilibrium quantity ΔF from a nonequilibrium measurement of the work.

We apply a time-dependent voltage $V_{PG}(t)$ to the plunger gate, which changes the energy of the electronic state in the QD from E_0 to E_1. The periodic voltage $V_{PG}(t)$ applied to the plunger gate, as shown in the inset of Fig. 4, consists of two sinusoidal parts, the drives, separated by a waiting time Δt allowing for equilibration of the QD. We distinguish between updrives $E_1^{up} > E_0^{up}$ and downdrives $E_0^{down} > E_1^{down}$.

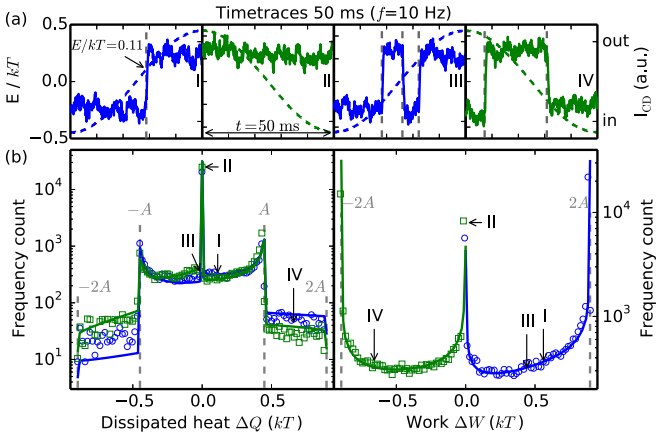

FIG. 3. Statistics of the heat dissipated in the reservoir and the work done on the quantum dot. (a) Examples of drive realizations in the upward (blue) and downward (green) direction, plotted as solid lines. The applied drive signals are shown as dashed lines. The driving is done by applying a voltage $V_{\rm PG} \propto -E$ to the plunger gate through an arbitrary waveform generator. From the position of the tunneling events (gray dashed lines), the heat and work of each realization are extracted. Bottom: The distribution for ΔQ (left) and ΔW (right) measured from approximately 20 000 realizations. Blue circles originate from upward drive and green squares from downward drive. The solid lines are rate equation calculations without free fitting parameters.

Frequency f and amplitude A of the sine determine the maximum steepness of the ramp.

During the drive we record the charge detector signal which provides the raw data for the following analysis of work, dissipation, and free energy. Figure 3(a) shows typical time traces $I_{\rm CD}(t)$ for four individual voltage ramps. When an occupied energy level of the QD is raised from well below the Fermi level up to an energy above the Fermi level, the electron leaves the QD on the way in most cases (panel I). For steep ramping, where the rise is fast compared to the tunneling rates, realizations without tunneling events become probable, as shown in panel II. Work is performed on the electron by the voltage source, if the driven QD level is occupied. For each realization, we determine the work ΔW performed on the QD from

$$\Delta W = \int_{E_0}^{E_1} n(E) dE, \tag{6}$$

where $n(E) \in \{0,1\}$ denotes the occupancy of the QD, as measured by the charge detector. For example, in realization I, with the drive applied symmetrically around $E = 0$, the electron is driven from $E_0^{(\rm up)} = -A = -0.45\ kT$ up to $E = 0.11\ kT$, where it leaves the QD. The work performed on the electron in the QD is therefore $\Delta W = (0.45 + 0.11)\ kT = 0.56\ kT$. Note that the maximum amount of work that can be performed on or by the QD system is given by $\pm 2A$.

For completeness, we also determine the heat ΔQ dissipated in the contact during each realization from the energies E_i of the QD state at which tunneling events occur. Each tunneling process contributes $\Delta Q_i = s_i E_i$, where s_i distinguishes between tunneling-out processes ($s_i = 1$) and tunneling-in processes ($s_i = -1$). This gives

$$\Delta Q = \sum_i E_i s_i, \ \Rightarrow\ |\Delta Q| \leqslant 2A. \tag{7}$$

After extracting ΔQ and ΔW from the single electron counting signal for each drive realization, we plot the probability distributions of ΔW and ΔQ in Fig. 3(b). Blue circles relate to driving upwards, green to downwards. With the tunnel rates given in Fig. 2(b), $\Gamma_{\rm in} = 42$ Hz and $\Gamma_{\rm out} = 21$ Hz, and drive parameters $f = 10$ Hz and $A = 0.45\ kT$, realizations as shown in panel II of Fig. 3(a), i.e., without tunnel events and hence zero dissipated heat, are very probable. This leads to the prominent delta peak at $\Delta Q = 0$ in Fig. 3(b). In these realizations, no work is done on the QD if the state stays empty during driving, leading to a peak at $\Delta W = 0$ in Fig. 3(b). If it is occupied, the work is $\Delta W = \pm 2A$ for upward or downward drive direction, respectively, giving rise to two additional peaks. Generally, the sharp features found in the probability distributions shown here are the signatures of nonequilibrium dynamics. The probability for intermediate dissipation $|Q| \sim 0$ increases for slower drives, and in close-to-equilibrium cases we find more Gaussian shaped distributions centered around zero dissipated heat (data not shown). This corresponds to the adiabatic limit, where a Gaussian distribution is expected, with a width given by the fluctuation-dissipation theorem [23], as discussed in more detail in Refs. [4,10]. Using the standard rate equation approach [4] with parameter values extracted from the equilibrium measurements [Fig. 2(b)], we calculate the probability distributions for the work and the dissipated

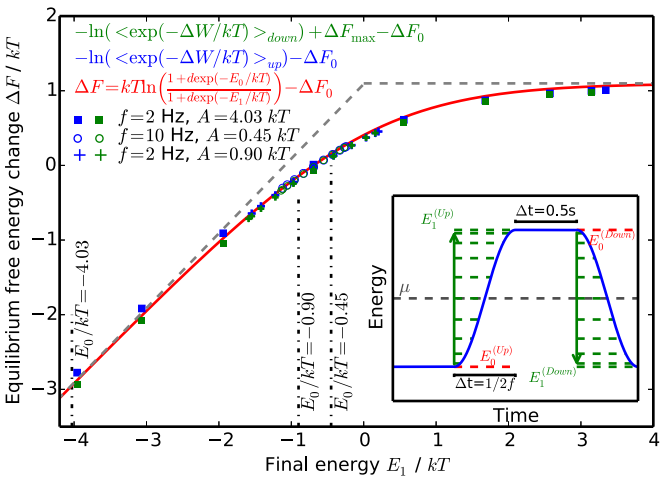

FIG. 4. The free energy of the QD during the drive, obtained with nonequilibrium measurement, measured with respect to the Fermi energy. Experimental results are plotted in green for the downward and in blue for the upward drive direction. Different markers denote independent experiments with different drive parameters. Each experiment consists of approximately 20 000 repetitions. The theory curve, Eq. (8), is plotted as a solid red line, for $d = 2$. Dashed gray lines indicate the expected linear increase at low E_1 as well as the saturation value for $E_1 > E_F$. Inset: One full period $-V_{\rm PG}(t) \propto E$ is plotted in blue. A waiting time of 0.5 s ensures thermal equilibration of the initial state. Green dashed lines indicate the values of E_1 for which we extract ΔF from the experiment.

heat in each drive direction [solid lines in Fig. 2(b)] and find very good agreement with the experimental data.

Utilizing Eq. (1), we now determine the equilibrium free energy change of the QD from the statistics of the performed work. The prerequisite that the initial state must be thermally equilibrated [1] is fulfilled by the waiting time. We determine the free energy change between the fixed initial and any freely chosen final state within the drive by analyzing ΔW, given in Eq. (6). As a result of Eq. (1) we get the free energy difference of the initial state and the chosen state within the drive. The change in free energy shown in Fig. 4 is determined along the full drive trajectory by varying the final state in the analysis. Different markers are used for the three measurements performed with the same gate configuration and QD resonance but with different values for A and f. Different colors distinguish upward and downward drive directions. Each of the six drive protocols gives an independent estimate for ΔF. From the extracted ΔW we also find that the average work always exceeds the free energy change, for large drive parameters and E_1 even by more than 100%. This identifies the nonequilibrium [1,14].

III. DISCUSSION

In equilibrium thermodynamics, the free energy is calculated from the difference of the partition sums of the initial ($i = 0$) and final ($i = 1$) states [14],

$$\Delta F = kT \ln\left(\frac{Z_0}{Z_1}\right), \quad Z_i = 1 + d \exp\left(\frac{-E_i}{kT}\right) \qquad (8)$$

We plot ΔF in Fig. 4 for $d = 2$ as a solid red line and observe a linear increase of the free energy in the first part of the drive, where the electron is lifted to an energy level still well below the Fermi energy. The increase in ΔF slows down around the Fermi energy, because the probability of the QD to be occupied decreases. At energies well above the Fermi level, the occupation probability approaches zero and the free energy saturates. The six independent measurements of ΔF agree well with the theoretical value along the whole drive trajectory.

Let us remind the reader that all parameters presented in Fig. 4 were directly derived from experimental data. The calculation of the free energy according to Eq. (8) used the degeneracy and temperature found from the equilibrium characterization and represents the right hand side of Eq. (1). The left hand side of the equation was extracted from charge detection time traces while driving the system. With our results, we experimentally confirm the validity of the JE for a full range of free energy values. This allows measuring the free energy of a driven system arbitrarily far from equilibrium.

In the original work by C. Jarzynski, an experimental test of Eq. (1) is suggested in a nanoscale system which is weakly coupled to a reservoir and evolves deterministically under its Hamiltonian [1]. Quantum extensions for the JE have been analyzed theoretically [24–27], and experimental results have been obtained recently [12]. In our work we have used a quantum system with a degenerate single-electron state evolving nondeterministically due to quantum tunneling. Nevertheless the work done on the system by the voltage source [Eq. (6)] is purely classical. According to Campisi [24], the Jarzynski equality is valid for classical or quantum systems in contact with a thermal heat bath and driven by classical forces. We have provided an experimental confirmation of this statement with our experiment.

Experimental limitations to the determination of the free energy are given by the stability of the sample as well as the bandwidth of the setup. The bandwidth limits the accuracy in the determination of the exact time of the tunnel event. Sample stability limits the number of repetitions which can be performed in a given configuration of the QD. In the experiment, we implement a feedback to align $E = 0$ to the Fermi level μ. Offsets due to drifts are taken into account in the analysis.

IV. CONCLUSION

In this paper we have shown that an equilibrium quantity, the free energy of a twofold degenerate single electron state, can be measured with an experiment driving the state far from equilibrium. Our results show how thermodynamic quantities such as work and dissipation can be understood on the microscopic level of individual quantum states and in nonequilibrium. The good agreement with theoretical calculations proves that we are able to control our QD-reservoir system with sufficient precision and that this system is well suited for studying out-of-equilibrium phenomena. Our work has identified a suitable system for studying the relation between thermodynamics and information theory. Investigating the influences of dissipation on fast qubit operations in quantum dot systems is a next step.

ACKNOWLEDGMENTS

We want to thank Jukka Pekola and Ivan Khaymovich for helpful discussions. We acknowledge the funding provided by the Schweizerischer Nationalfonds (SNF) and Quantum Science and Technology (QSIT), which enabled this work.

[1] C. Jarzynski, Phys. Rev. Lett. **78**, 2690 (1997).
[2] G. E. Crooks, Phys. Rev. E **60**, 2721 (1999).
[3] D. Collin, F. Ritort, C. Jarzynski, S. B. Smith, I. Tinoco, and C. Bustamante, Nature (London) **437**, 231 (2005).
[4] O.-P. Saira, Y. Yoon, T. Tanttu, M. Möttönen, D. V. Averin, and J. P. Pekola, Phys. Rev. Lett. **109**, 180601 (2012).
[5] J. Liphardt, S. Dumont, S. B. Smith, I. Tinoco, and C. Bustamante, Science **296**, 1832 (2002).
[6] B. Küng, C. Rössler, M. Beck, M. Marthaler, D. S. Golubev, Y. Utsumi, T. Ihn, and K. Ensslin, Phys. Rev. X **2**, 011001 (2012).
[7] D. M. Carberry, J. C. Reid, G. M. Wang, E. M. Sevick, D. J. Searles, and D. J. Evans, Phys. Rev. Lett. **92**, 140601 (2004).

[8] V. Blickle, T. Speck, L. Helden, U. Seifert, and C. Bechinger, Phys. Rev. Lett. **96**, 070603 (2006).
[9] G. M. Wang, E. M. Sevick, E. Mittag, D. J. Searles, and D. J. Evans, Phys. Rev. Lett. **89**, 050601 (2002).
[10] F. Douarche, S. Ciliberto, A. Petrosyan, and I. Rabbiosi, EPL **70**, 593 (2005).
[11] J. V. Koski, T. Sagawa, O.-P. Saira, Y. Yoon, A. Kutvonen, P. Solinas, M. Möttönen, T. Ala-Nissila, and J. P. Pekola, Nat. Phys. **9**, 644 (2013).
[12] S. An, J.-N. Zhang, M. Um, D. Lv, Y. Lu, J. Zhang, Z.-Q. Yin, H. T. Quan, and K. Kim, Nat. Phys. **11**, 193 (2015).
[13] T. B. Batalhão, A. M. Souza, L. Mazzola, R. Auccaise, R. S. Sarthour, I. S. Oliveira, J. Goold, G. De Chiara, M. Paternostro, and R. M. Serra, Phys. Rev. Lett. **113**, 140601 (2014)
[14] L. Reichl, *A Modern Course in Statistical Physics* (Arnold, London, 1980).
[15] R. Hanson, L. P. Kouwenhoven, J. R. Petta, S. Tarucha, and L. M. K. Vandersypen, Rev. Mod. Phys. **79**, 1217 (2007).
[16] M. Ciorga, A. S. Sachrajda, P. Hawrylak, C. Gould, P. Zawadzki, S. Jullian, Y. Feng, and Z. Wasilewski, Phys. Rev. B **61**, R16315 (2000).
[17] S. Tarucha, D. G. Austing, T. Honda, R. J. van der Hage, and L. P. Kouwenhoven, Phys. Rev. Lett. **77**, 3613 (1996).
[18] R. Schleser, E. Ruh, T. Ihn, K. Ensslin, D. C. Driscoll, and A. C. Gossard, Appl. Phys. Lett. **85**, 2005 (2004).
[19] L. M. K. Vandersypen, J. M. Elzerman, R. N. Schouten, L. H. W. v. Beveren, R. Hanson, and L. P. Kouwenhoven, Appl. Phys. Lett. **85**, 4394 (2004).
[20] S. Gustavsson, R. Leturcq, B. Simovic, R. Schleser, T. Ihn, P. Studerus, K. Ensslin, D. C. Driscoll, and A. C. Gossard, Phys. Rev. Lett. **96**, 076605 (2006).
[21] C. G. Darwin, Math. Proc. Cambridge Philos. Soc. **27**, 86 (1931).
[22] V. Fock, Z. Phys. **47**, 446 (1928).
[23] H. Nyquist, Phys. Rev. **32**, 110 (1928).
[24] M. Campisi, P. Talkner, and P. Hänggi, Phys. Rev. Lett. **102**, 210401 (2009).
[25] P. Talkner and P. Hänggi, J. Phys. A: Math. Theor. **40**, F569 (2007).
[26] T. Albash, D. A. Lidar, M. Marvian, and P. Zanardi, Phys. Rev. E **88**, 032146 (2013).
[27] A. E. Rastegin and K. Zyczkowski, Phys. Rev. E **89**, 012127 (2014).